Astrophysical Opacity

Forrest J. Rogers and Carlos A. Iglesias

An array of problems in astronomy, cosmology, and particle physics is dependent on our understanding of the evolution and structure of stars. Stellar structure and evolution, in turn, depend on how the nuclear energy generated in the stellar center is transported to the surface. Energy transport by photons is a primary transfer mechanism. Recent improvements in the calculation of the radiative properties of stellar matter have helped resolve several long-standing discrepancies between observations and the predictions of theoretical models.

Stellar interiors are immense nuclear furnaces that synthesize elements and convert matter into energy. The physical properties of stars depend on the transport of energy to the stellar surface (*1*). This can occur by conduction, convection, or radiation, but of these, radiation is the most important. The efficient transport of energy by photons depends on the transparency of the intervening matter to radiation flow, or the radiative opacity. The ultimate impact of radiative opacity goes well beyond its role in stellar modeling because the properties of stars are used to estimate the age and density of the universe, determine intergalactic distances, understand the big bang nucleosynthesis, investigate the evolution of the elemental composition of galaxies, and constrain the properties of nonbaryonic matter.

Stellar evolution occurs over long time scales that depend strongly on the initial mass available to form the star, proceeding more rapidly in higher mass stars. The time required for gravitational contraction of a gas cloud having the mass of the sun to the current solar diameter, known as the Kelvin-Helmholtz time, is about 10 million years, and the time required for quasi-stable burning of the nuclear fuel is about 10 billion years. During this time, nuclear fusion changes the interior composition, and the resulting changes in the equation of state and opacity drive a gradual evolution in the structure. Geologic evidence is consistent with this picture, suggesting that the sun has not changed appreciably for at least the past billion years. More generally, the observation of other stars reveals that most are in both hydrostatic and thermal equilibrium: Gravitational forces are balanced by pressure forces, and the energy generated by nuclear burning in the core is balanced by the energy being radiated from the surface. The mean free path of photons emitted in stellar cores is on the order of centimeters, so that a very large number of absorptions and reemissions must occur before the energy carried by the photon reaches the surface (in about the Kelvin-Helmholtz time). The efficiency of this energy transfer is related to the temperature gradient, which is directly proportional to the mean radiative opacity in radiation-dominated regions. When the radiative opacity is large, convection can become the more efficient energy transport mechanism.

Photoabsorption is usually described by three processes. Continuous absorption occurs when the final electronic state is in the continuum. This can occur either by photoionization (bound-free transition), when the active electron originates from a bound state, or by inverse bremsstrahlung (free-free), when the active electron also originates from a scattering state. When both the original and final state of the active electron are bound states, discrete line radiation (bound-bound) occurs. The third type of process, electron scattering, is not true photoabsorption. In this process, a photon is absorbed by a free electron and then immediately radiated in some other direction, thus effectively removing energy from the photon beam.

The radiation transfer equation describes the transport of energy by photons and is equivalent to the Boltzmann equation in the kinetic theory of particle transport (*2*). In stellar interiors, where conditions change slowly over many photon mean free paths and stellar matter is close to local thermodynamic equilibrium, the transfer equation is greatly simplified. In this limit, known as the diffusion approximation, the monochromatic absorption appearing in the transfer equation can be replaced with a flux-gradient mean

$$\frac{1}{\kappa_R} = \int_0^\infty d\nu \frac{1}{\kappa(\nu)} \frac{dB_\nu}{dT} \Bigg/ \int_0^\infty d\nu \frac{dB_\nu}{dT} \qquad (1)$$

where dB_ν/dT is the derivative of the Planck function with respect to temperature, $\kappa(\nu)$ is the total extinction coefficient, including stimulated emission plus scattering, and κ_R is the Rosseland mean opacity or simply the opacity. A large value of the opacity indicates strong absorption from a beam of photons, whereas a small value indicates that the beam loses very little energy as it passes through the medium.

Early opacity calculations assumed that bound-bound absorption was unimportant, and only the continuous and scattering processes were included. A review of the early work on opacity is given by Cox (*3*), who was involved in the first major effort to include bound-bound absorption in astrophysical opacity calculations (*4*). The bound-bound absorption was found to be a major source of opacity in regions where stellar matter is partially ionized. For the heavier elements, like iron, this region extends all the way down to the stellar core. Continued revisions and extensions of this work (*5, 6*) culminated in the Los Alamos Astrophysical Opacity Library (*6*) and the results have been instrumental in understanding the main features of stellar evolution.

However, a number of observable phenomena that are sensitive to opacity resisted theoretical explanation. For example, some observed properties of pulsating stars could not be explained, and the observed lithium abundance of low mass stars in the Hyades cluster is much less than that of the interstellar matter from which the stars were formed. Closer to home, the measured neutrino flux from the sun has been persistently about one-third of that calculated by standard solar models (*7*). In the latter case, it now appears that particle physics may be the solution to the problem. A likely explanation is the Mikeyev, Smirov, and Wolfenstein effect, where electron neutrinos undergo a transformation by interaction with the solar material to change to muon or tauon flavors (*8*). The sun and stars have, therefore, become tools with which we can test the properties of neutrinos and other exotic matter candidates. Standard stellar models with good opacities are needed to assess whether the new particle physics ideas are compatible with established criteria. In addition, models of the sun's seismic activity depend critically on the input opacities (*9*).

Many stars, including the sun, are on what is known as the hydrogen-burning main sequence, or more commonly, just the main sequence. Main sequence stars are in a quasi-stable process of burning hydrogen into helium in their deep interiors. During this phase of their evolution, all such stars occupy a narrow region in a plot of lumi-

The authors are at the Lawrence Livermore National Laboratory, Livermore, CA 94550.

nosity versus spectral class (or surface temperature). Such plots are called Hertzprung-Russell or HR diagrams after their originators. Stars on the main sequence are composed of mostly hydrogen and helium with only a small amount of heavier elements, called "metals" by astronomers. Because of nucleosynthesis in earlier stellar generations, relatively young stars are made from matter that is metal-rich, typically about 2% metals by mass. Metallicity varies considerably among different stellar age populations in galaxies. Older stars, whose matter has not been recycled as much in previous stellar generations, have typically one to two orders of magnitude lower metal content. To understand the history of how these different stellar populations were formed, we must understand the effects of metallicity, particularly how it influences the opacity, which is very sensitive to the heavy element content because the number of available atomic transitions increases with atomic number.

With the exhaustion of hydrogen in the deep interior, stars enter more advanced stages of evolution. They become red giant stars, burning hydrogen in a shell around their inactive helium cores. Eventually, most burn helium into carbon by the triple alpha process in which three helium nuclei collide to form a carbon nucleus. Because of their location in the HR diagram during this stage of evolution, such stars are generally called horizontal branch or HB stars, and at higher masses, blue loop stars. As the helium burning continues, the luminosity and surface temperature change, and the star continues to move in the HR diagram. The details of the evolutionary track depend on the initial stellar mass and elemental composition. For example, intermediate mass stars (3 to 8 $M_\odot$, where $M_\odot$ is one solar mass) eventually exhaust their interior helium and evolve along the asymptotic branch of the HR diagram (*1*). Quantification of the opacity for these wide-ranging conditions is a basic requirement for stellar modeling.

It was noticed early that an artificial increase of the opacity at certain temperatures and densities could substantially improve the agreement between theory and observationally determined period ratios of variable stars (*10*), but the increases needed seemed to be so large that no possible photoabsorption mechanism seemed plausible. It was Simon (*11*), however, who gave the most compelling arguments for reexamining the metal contribution to the opacity. He showed that increasing this contribution, so that the total opacity is increased by a factor of 2 or 3 in the few hundred thousand degree temperature range, could resolve the period ratio problem. Our group at Lawrence Livermore National Laboratory was the first to respond with new opacity calculations based on improved equation of state and atomic physics (*12, 13*); we refer to our effort as OPAL. More recently, opacity calculations by the Opacity Project (OP) have also become available (*14*) for stellar envelopes. Because of the earlier availability of the OPAL opacities, they have been used in most of the new modeling studies.

Opacity

The major source of the opacity increases has been the use of improved atomic physics in the calculations. There are several possible levels of detail for atomic data; take, for example, the transitions that connect two electrons in an *sp* configuration to a p^2 configuration through a one-electron jump (Fig. 1). In the simplest case, all transitions are assumed to have the same energy. Opacity calculations that carry out a sum over a large number of configurations in this approximation are referred to as detailed configuration accounting (DCA) methods. However, the DCA approach neglects nonspherical interactions that remove the degeneracy and lead to configuration term structure. The calculation of the nonspherical terms has developed into a powerful algebra (*15*) that couples orbital (L) and spin (S) angular momentum states. In light elements, the dominant nonspherical term is the Coulomb interaction between the electrons, which leads to pure *LS* coupling. In *LS* coupling, the single spectral line of the DCA method (Fig. 1) is split into three distinct lines, corresponding to a triplet and two singlet terms. With heavier

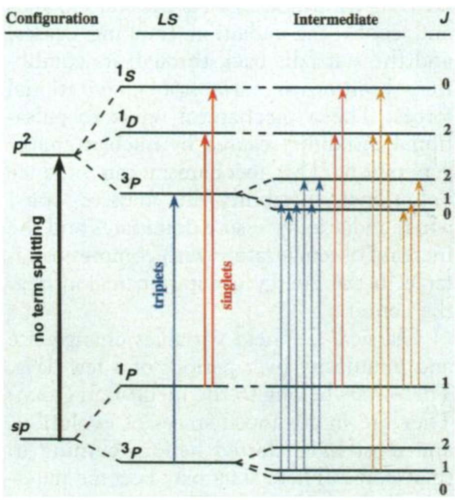

Fig. 1. Transitions from *sp* up to p^2 in various approximations. The black arrow shows the configurational average transition (DCA approximation). The colored arrows show the allowed transitions in the *LS* and intermediate coupling schemes: red, singlets (S = 0); blue, triplets (S = 1); and amber, intercombination lines. Total angular momentum of the state, J.

elements, such as those in the iron group, the interaction between the electron spin and the magnetic field resulting from the electron orbital motion is no longer negligible and requires intermediate coupling (*15*). In intermediate coupling, the three lines of the *LS* coupling scheme blossom into eight lines having no net total spin change, $\Delta S = 0$, and six intercombination lines having $\Delta S = \pm 1$. In more complicated configurations, the increase in the number of spectral lines can be more dramatic.

The Los Alamos calculations (*3–6*) were mostly based on the DCA method. In response to Simon's plea for reexamination of the metal contribution to astrophysical opacities (*11*), a group at Los Alamos investigated the effect of including more detailed atomic data (*16*). They concluded that it would not change their results by more than 30%, much less than was needed to resolve the puzzles in pulsation theory. In particular, they concluded that transitions between states with the same principal quantum number, not included in the Los Alamos calculations, are not a significant source of opacity.

Because of the importance of opacity to many facets of stellar modeling, the Los Alamos study notwithstanding, the OPAL and OP groups undertook completely new, independent efforts to calculate astrophysical opacities. Contrary to the conclusions of the Los Alamos group (*16*), preliminary OPAL results showed substantial increases in opacity (*12*), up to a factor of 4 in more complete calculations (*13, 17*). These increases were largely a result of the rich spectrum of transitions originating in the M shell of iron, with an important contribution from the intra–M shell transitions neglected by Los Alamos (*3–6*). The largest increases in κ_R occur in the few hundred thousand degree range, where the energies of these lines are near the maximum in dB_ν/dT in Eq. 1. It also was found that full intermediate coupling was necessary (*18*). Similar results have been obtained by the OP group (*14, 19*). The importance of iron as a contributor to astrophysical opacity was overlooked in earlier work because the fractional mass content of iron in stellar plasmas is only about 10^{-5} and its potential for filling in areas of weak absorption in the Rosseland integral (Eq. 1) was not fully appreciated.

Accurate models of stellar structure require detailed computer calculations. However, in regions where radiation pressure dominates, the ratio of the matter pressure to the radiation pressure is approximately constant (*1*). Using the nonrelativistic ideal gas pressure in combination with the Stefan-Boltzmann law, one obtains with the above assumption a constant value for ρ/T^3, where ρ is density and T is temperature. Thus, it is convenient to tabulate the Rosseland mean opacity at constant values of R against temperature, where $R = \rho/T_6^3$, ρ is in grams per cubic centimeter, and T_6 is the temperature in millions of degrees kelvin.

When the opacity is plotted as a function of temperature for constant R (Fig. 2), the curves show a series of bumps in log κ_R that are caused by strong absorption features in the spectrum. The H, He, and He^+ bumps (Fig. 2) long have been associated with pulsational driving in variable stars (*1*). However, the substantial bump in the new opacities around log $T = 5.4$ is missing in the earlier results. This new bump, attributable mostly to absorption in iron, resolves several long-standing pulsation problems. The bump near log $T = 6.3$ is important to helioseismology as well as lithium depletion in low mass stars.

A major reason that large deficiencies in the astrophysical opacities persisted over such a long time was the lack of laboratory experiments to test the theory. New experimental techniques involving laser-heated samples are changing this situation (*20*). Recent experiments with iron foils (*21*) have produced plasmas with temperatures near 250,000 K and densities around 0.008 g/cm^3, conditions comparable to those in the pulsational driving region of classical Cepheids. These experiments measure the transmission through the iron, which is related to the photoabsorption according to $e^{-\rho L \kappa(\nu)}$, where L is the foil thickness. The experimental results are compared with two versions of OPAL in Fig. 3. A DCA version, which approximates the Los Alamos calculations (*4*–*6*), shows only weak absorption for photon energies around 70 eV, whereas both of the calculations with full intermediate coupling and the experiment show strong absorption in this spectral region. The intrashell transitions make a strong contribution to this absorption feature. This was the first direct experimental test of the new opacities. A second experimental group has since measured the iron transmission over a sufficiently broad range to obtain the Rosseland average (*22*); again, good agreement was found between theory and experiment.

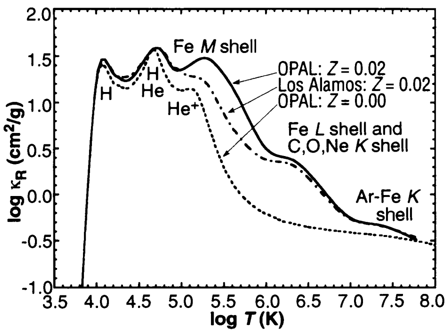

Fig. 2. Opacity versus temperature for a 15-element mixture of solar composition along a track of constant R (log $R = -3$). The mixture has a hydrogen mass fraction $X = 0.7$. The OPAL results are shown for metal mass fractions $Z = 0$ and 0.02, corresponding to helium mass contents of $Y = 0.3$ and 0.28, respectively. The results for a commonly used set of Los Alamos opacities (*5*) with $Z = 0.02$ are also plotted.

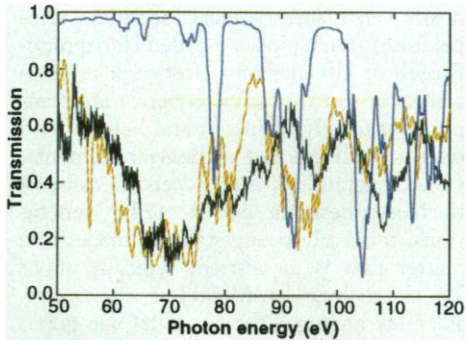

Fig. 3. The Fe transmission experiment (black line) (*21*) compared with OPAL results calculated with intermediate coupling (amber line) and in DCA with hydrogenic oscillator strengths (blue line).

Pulsating Stars

Under the right driving conditions, stars can undergo large radial pulsations, much like the standing waves of a rope that is fastened at both ends. Once some driving mechanism displaces it from its equilibrium position, pressure forces push outward when the stellar radius is too small, and gravitational forces pull it back when it is too large. Because of the damping that results from the exchange of energy between different layers of the star, such excitations exist only over relatively brief intervals in the lifetime of a star when it is in an instability region of the HR diagram.

Two primary mechanisms have been proposed for exciting large amplitude radial oscillations. They have distinct characteristics that can be categorized and have been given the names κ and ε mechanisms (*1*). The κ mechanism occurs in regions where the opacity rises sharply with increasing temperature in ionization zones. Under such conditions, a contraction of the star can increase the opacity in this region, trapping the energy flux emanating from the interior. The trapped energy further increases the temperature and pressure, causing an expansion of the star and increasing its brightness. As the star expands and cools, the radiation trapping ceases, and the star falls back through its equilibrium position as a result of gravitational forces. The ε mechanism refers to pulsational instability caused by nuclear energy generation. This mechanism can produce pulsational instability in massive stars, where radiation pressure dominates and the increase of temperature with compression is large in the energy generation region near the center.

Classical Cepheid variables change size and luminosity over periods of a few days. These stars belong to the metal-rich group. They are in advanced stages of evolution, and most have started helium burning in their cores. These stars may become pulsationally unstable several times during their lifetime. Pulsational instability in these stars is driven by the κ mechanism operating in the He^+ ionization zone. Remarkably, when Henrietta Leavitt studied classical Cepheids at the Harvard College Observatory, she discovered in 1908 that they display a strong correlation between their pulsation period and luminosity. This simple relation provides one of the most reliable methods for the determination of distances to nearby galaxies and is frequently used to calibrate distances of remote galaxies (*23*). It is the measurement of the velocity-distance relation for remote galaxies that gives an estimate for the age of the universe.

Some Cepheid variables display pulsation in several modes, and the period ratios are sensitive to the stellar mass. However, a long-standing controversy has existed because masses deduced from pulsation models that match the observed period ratios are as much as 50% lower than those obtained from stellar evolution theory. Besides the periods, the brightness magnitude and radial velocity as a detailed function of time are also observed. The resulting curves are different for different types of Cepheids. The "bump" Cepheids, which have periods of around 10 days, display a luminosity curve that changes systematically with increasing period. This phenomenon is a consequence of a 2:1 resonance between the second overtone and the fundamental mode that is sensitive to the stellar mass. The "beat" Cepheids pulsate with one period whose amplitude changes periodically with a longer period. This beat phenomenon results from the superposition of two modes of slightly different period (*1*).

Moskalik, Buchler, and Marom (*24*) were the first to analyze classical Cepheid masses using new opacities that include a realistic treatment of bound-bound absorption in iron. They obtained good agreement with other methods of mass determination for the double mode Cepheids. In a Petersen diagram (Fig. 4), their results lie in the same region as the observed data and have similar slope, whereas calculations made with the Los Alamos opacities (*5*) lie far from the observations. The predicted masses for bump Cepheids also increased and are now comparable to evolutionary masses. A previously

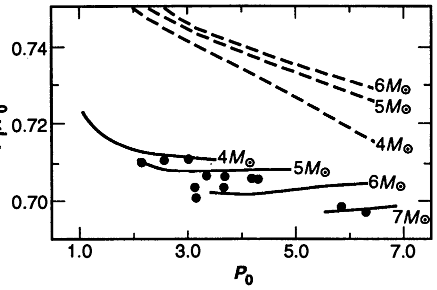

Fig. 4. Petersen diagram of the ratio of the period for the first overtone, P_1, to that of the fundamental mode, P_0. The dots represent observational data for individual stars, and the curves give loci for the theoretical models corresponding to the indicated mass in solar units: Los Alamos (*5*) (dashed lines); OPAL (solid lines). [Reprinted from (*24*) with permission]

unseen large sensitivity of the period ratios to luminosity and metallicity, which could provide new observational tests for opacity, was also found. Similar results have been reported in a more recent study (*25*).

The metal-poor RR Lyrae stars are located in the Cepheid instability strip of the HR diagram and also display large radial oscillations. The RR Lyrae stars are less massive than the classical Cepheids and have somewhat shorter periods, typically around half a day. They separate into two groups of different metallicity called Oosterhoff I and II. The RR Lyrae stars are found throughout the galaxy, but are more common in the galactic halo and are frequently observed in globular clusters. Again, the masses of the RR Lyrae stars as determined from pulsation theory have been significantly less than those predicted by evolution theory. Because of their much lower metal content, it was not expected that the new opacities would have much effect on the model calculations. However, even for these low metallicity stars, opacity increases of up to 50% were obtained. In this case, not only are the increased opacities attributable to metals important, but decreases in opacity for temperatures below 100,000 K also increase the masses (*26*). This decrease in opacity results from an improved treatment of the hydrogen spectral lines, which reduces the contribution from the far wings (*17*). The opacity decrease in conjunction with a modest opacity increase from the metals at a higher temperature eliminates the inconsistency between masses in the two globular cluster types as well as between pulsation and evolution theory (*26*). Similar mass anomalies in other stars displaying Cepheid-type variability have been successfully explained with the new opacities (*27*). A concern, however, is that the improved opacities may alter theoretical evolutionary masses, particularly those of the horizontal branch stars found in globular clusters. Recent calculations (*28*) show that the changes in the deduced masses of HB stars are not significant.

The globular cluster stars are of special interest because they are among the oldest objects in the universe. They play an important role in the establishment of a lower limit to the age of the universe and in the understanding of the origin and evolution of the galaxy (*29*). This limit has important implications for cosmological theories because the universe has to be older than the objects it contains by at least the time it took for the objects to form. Determination of the ages of globular cluster stars depends on knowledge of their distance and luminosity as well as the abundance ratio of certain elements, particularly oxygen and iron. Current estimates for the ages of globular cluster stars range from about 13 billion to 17 billion years (*23*). These ages are consistent with the expansion time scale of the universe only if the expansion rate, H_0, known as the Hubble constant, and the ratio of the present density of the universe to the closure density, Ω_0, fall within a certain range. There is considerable controversy over the value of these constants. Measured values of H_0 are clustered around the two values 50 and 80 km s^{-1} Mpc^{-1}. The controversy arises because the lower value of H_0 suggests an age of 15 billion to 20 billion years, whereas if Ω_0 is equal to unity, as is implied by current cosmological theory with inflation (*30*), the higher value suggests an age of under 10 billion years. The smaller age is much less than that estimated for globular cluster stars. Many attempts to measure Ω_0 imply values somewhat less than unity, indicating that the universe will continue to expand forever. The ages of globular clusters thus provide an important constraint on H_0 and Ω_0.

The globular cluster ages are also important as they relate to galaxy formation. They appear to be much older than the disk of our galaxy and contain fewer products of stellar nucleosynthesis. Thus, distributions of the age and elemental composition of globular clusters provide important clues to the early epochs of star formation that preceded the formation of the disk of our galaxy.

Another long-standing puzzle in pulsation theory has been determination of the driving mechanism for pulsation in some B stars, called β Cephei stars. These stars have masses 10 to 20 times that of the sun and lie outside of the Cepheid instability strip near the upper end of the main sequence. In the Cepheid mass problem discussed above, the driving mechanism was not the issue. Instead, the problem was how to obtain the correct pulsation periods. In the case of the β Cephei stars, the κ mechanism driving with the Los Alamos opacities (*4–6*) was too weak to drive pulsations, and many unconventional methods to produce instability were tried unsuccessfully (*31*). The strong increase in absorption starting at temperatures above 100,000 K, absent in all previous opacity calculations, again provides the missing piece of the puzzle (*32*). This κ mechanism instability is sensitive to iron content, and the star-to-star variability in iron abundance may explain why only some B stars pulsate. The sensitivity to the iron may also be responsible for the lack of observed pulsating B stars in the relatively iron-poor Magellanic clouds (*33*).

Nuclear-energized pulsational instability (ε mechanism) has been a well-known feature of models of chemically homogeneous massive stars. Earlier estimates of the minimum critical mass for the onset of this instability were inconsistent with the observed lack of pulsation in the brightest O stars at the upper end of the main sequence. The high radiation pressure and relatively low density near the stellar center only produce instability in the fundamental mode. The damping of this mode, however, occurs near the surface and is sensitive to the opacity. Recent studies with the new opacities have obtained somewhat different results for the effect on the fundamental mode: Stothers (*34*) found that the minimum mass required for pulsation is above those of the largest observed O stars, whereas Glatzel and Kiriakidis (*35*) obtained results similar to earlier studies.

Pulsations have recently been observed in Wolf-Rayet stars (*36*). These stars are helium burners and are among the most luminous stars observed. They exhibit broad emission bands corresponding to carbon or nitrogen and are losing mass at a very high rate. Recent model calculations indicate that, because of a combination of ε- and κ-mechanism driving, these stars should become pulsationally unstable for masses around 14 to 20 $M_\odot$ (*34, 35*). The large iron opacity is again a factor.

Helioseismology

Variations in the Doppler velocity of the solar surface were first observed by Leighton (*37*) in 1960. The source of these variations was later determined to be resonant acoustic oscillations in a limited region below the solar surface (*38*). Typically, the variations have a 5-min period and are called *p* modes to reflect that they are caused by pressure variations. It is now well established that low-frequency *p* modes probe deep into the solar interior and can help determine the depth of the convection zone, initial solar helium abundance, as well as differential rotation with both depth and latitude. Theoretical models of these properties depend sensitively on input physics, such as the equation of state, element diffusion, and opacity. Discrepancies between observation and calculation are thus indirect tests of the input physics and have already anticipated deficiencies in some of these quantities.

Several groups noticed that increases in the Los Alamos (6) opacities of 10 to 20% in the few million degree temperature range, just below the bottom of the solar convection zone, would improve agreement of the calculated *p*-mode frequencies with observations (*39, 40*). This was borne out by new opacity results (*41*), which are 10 to 15% larger in this temperature region and have played a key role in improving the solar models. For example, helioseismic observations revealed changes in the sound speed that place the inner boundary of the convection zone at 0.713 ± 0.003 solar radii (*42*). Recent calculations (*43*) with the latest input physics now obtain close agreement with these observations. In addition to the opacity, the treatment of element diffusion had significant impact on the model calculations (*40, 43, 44*).

Lithium Depletion

Lithium is a key nucleus in the understanding of big bang nucleosynthesis. It is estimated that just after the big bang, primordial matter had a ^{7}Li fractional mass content of about 10^{-7}. The reaction $^6\mathrm{Li} + {}^1\mathrm{H} \rightarrow {}^4\mathrm{He} + {}^3\mathrm{He}$ occurs at temperatures above 2.0×10^6 K, and the reaction $^7\mathrm{Li} + {}^1\mathrm{H} \rightarrow 2{}^4\mathrm{He}$ takes place at temperatures above 2.4×10^6 K. Models of the sun and hotter stars predict that the convection zone extends down to about the 2 million degree region, but not as deep as 2.4 million degrees. Consequently, convective mixing of the lithium from above should destroy the ^{6}Li in these stars, but not the ^{7}Li. No ^{6}Li is observed, but the ^{7}Li for the sun and some nearby stars in the HR diagram are depleted by about a factor of 100 compared with meteorites and the most lithium-rich stars. This suggests that other mechanisms are at work. One often proposed mechanism is convective overshooting, where the boundary between the convection and radiation zones is not sharp; that is, falling bubbles arrive at the lower edge of the convection zone with a lower temperature and higher density than their surroundings and penetrate some distance into the radiation zone before coming to rest. However, with the new opacities, the need for overshooting in other areas of stellar evolution has been greatly reduced if not eliminated (*45*). The cause for solar lithium depletion remains unresolved. In other younger, somewhat cooler main sequence stars, such as those found in the Hyades cluster, the base of the convection zone is still not expected to be hot enough to burn ^{7}Li. Hyades stars of mass similar to that of the sun have also apparently depleted their ^{7}Li by about a factor of a 100. Attempts over the past three decades to explain this depletion have not been entirely successful. One possibility is that the lithium was destroyed during early stages of evolution before these stars settled down on the main sequence, but early attempts to explain the lithium depletion this way failed. However, noting a historical trend toward increased opacity in the few million degree range, Swenson, Stringfellow, and Faulkner (*46*) determined that a 37% increase in the Los Alamos opacities (*5*) could solve the puzzle. The new opacity results do in fact provide substantial opacity increases and improve the agreement with observation for the Hyades cluster stars (*47*). The behavior of the lithium abundance observed for different types of stars suggests that other lithium-depletion mechanisms may also be at work (*48*).

Prospects for the Future

The applications of the new opacities have so far concentrated on main sequence and helium-burning post–main sequence stars. It remains to be seen what the effects of the new opacity will be on more evolved stars that have exhausted most of their core hydrogen and perhaps even their helium. Depending on their initial mass and metallicity, these stars can display a wide range of phenomena, ending up as exploding supernova in one extreme or as cooling white dwarfs in the other. Modeling of many of these phenomena also depends on the opacity and will require extension of the calculations to higher densities and metallicities (*49*).

Cool stars with surface temperatures below 5000 K can form a wide variety of molecules in their atmospheres. Molecular opacities in these stars affect the surface temperature and are important for determination of their masses. A substantial part of the mass in the galaxy may be locked up in low mass, cool stars, and reliable opacities are needed to answer this question. Several groups are in the process of improving molecular opacities, and new results are just becoming available (*50*).

Now that basic methods for the measurement of photoabsorption and opacity in laser-produced plasmas have been developed, it can be expected that experiment will play a more important role in future research. Experiments on shock-produced plasmas also promise to provide data in the higher density, low-temperature white dwarf region (*51*).

REFERENCES AND NOTES

1. E. Bohm-Vitense, *Introduction to Stellar Astrophysics* (Cambridge Univ. Press, Cambridge, 1992), vols. 2 and 3.
2. D. Mihalas, *Stellar Atmospheres* (Freeman, San Francisco, CA, 1978).
3. A. N. Cox, *Stellar Structure*, vol. 8 of *Stars and Stellar Systems*, L. H. Aller and D. B. McLaughlin, Eds. (Univ. of Chicago Press, Chicago, 1965), p. 185.
4. ______ and J. N. Stewart, *Astron. J.* **67**, 113 (1962).
5. A. N. Cox and J. E. Tabor, *Astrophys. J. Suppl. Ser.* **31**, 271 (1976).
6. W. F. Huebner, A. L. Merts, N. H. Magee, M. F. Argo, *Los Alamos Sci. Rep. La-6760-M* (1977).
7. J. N. Bahcall and R. K. Ulrich, *Rev. Mod. Phys.* **60**, 297 (1988).
8. M. Cherry, *Nature* **347**, 708 (1990).
9. W. A. Dziembowski, A. A. Pamyatnykh, R. Sienkiewicz, *Acta Astron.* **14**, 5 (1992).
10. K. Fricke, R. S. Stobie, P. A. Strittmatter, *Mon. Not. R. Astron. Soc.* **154**, 23 (1971); J. O. Petersen, *Astron. Astrophys.* **34**, 309 (1974); W. B. Stellingwerf, *Astrophys. J.* **83**, 1184 (1978).
11. N. R. Simon, *Astrophys. J.* **260**, L87 (1982).
12. C. A. Iglesias, F. J. Rogers, B. G. Wilson, *ibid.* **322**, 145 (1987).
13. C. A. Iglesias and F. J. Rogers, *ibid.* **371**, L73 (1991).
14. M. J. Seaton, Y. Yan, D. Mihalas, A. K. Pradhan, *Mon. Not. R. Astron. Soc.*, in press.
15. R. D. Cowan, *The Theory of Atomic Structure* (Univ. of California Press, Berkeley, CA, 1981).
16. N. H. Magee, A. L. Merts, W. F. Huebner, *Astrophys. J.* **283**, 264 (1984).
17. F. J. Rogers and C. A. Iglesias, *Astrophys. J. Suppl. Ser.* **79**, 507 (1992).
18. C. A. Iglesias, F. J. Rogers, B. G. Wilson, *Astrophys. J.* **397**, 717 (1992).
19. Y. Yan, *Rev. Mex. Astron. Astrofis.* **23**, 171 (1992).
20. T. S. Perry *et al.*, *Phys. Rev. Lett.* **67**, 3784 (1991).
21. L. B. DaSilva *et al.*, *ibid.* **69**, 438 (1992).
22. P. T. Springer *et al.*, *ibid.*, p. 3735.
23. W. L. Freedman, *Sci. Am.* **267**, 54 (November 1992).
24. P. Moskalik, J. R. Buchler, A. Marom, *Astrophys. J.* **385**, 685 (1992).
25. S. M. Kanbur and N. R. Simon, *ibid.*, in press.
26. A. N. Cox, *ibid.* **381**, L71 (1991); G. Kovacs, J. R. Buchler, A. Marom, *Astron. Astrophys.* **252**, L27 (1992).
27. J. O. Petersen, *ibid.* **265**, 555 (1992).
28. S. Yi, Y.-W. Lee, P. Demarque, *Astrophys. J.* **411**, L25 (1993).
29. R. J. Taylor, *Q. J. R. Astron. Soc.* **27**, 367 (1986).
30. A. H. Guth and P. J. Steinhardt, *Sci. Am.* **250**, 116 (May 1984).
31. A. N. Cox, in *Stellar Pulsation*, A. N. Cox, W. M. Sparks, S. G. Starrfield, Eds., vol. 274 of *Lecture Notes in Physics* (Springer-Verlag, New York, 1987), p. 36.
32. ______, S. B. Morgan, F. J. Rogers, C. A. Iglesias, *Astrophys. J.* **393**, 272 (1992); M. Kiriakidis, M. F. El Eid, W. Glatzel, *Mon. Not. R. Astron. Soc.* **255**, 1 (1992); P. Moskalik and W. A. Dziembowski, *Astron. Astrophys.* **256**, L5 (1992).
33. L. A. Balona, *Mon. Not. R. Astron. Soc.* **251**, 66 (1992); C. Waelkens, K. Van den Abeele, H. Van Winckel, *Astron. Astrophys.* **251**, 69 (1991).
34. R. B. Stothers, *Astrophys. J.* **392**, 706 (1992); ______ and C.-w. Chin, *ibid.* **408**, L85 (1993).
35. W. Glatzel and M. Kiriakidis, *Mon. Not. R. Astron. Soc.* **262**, 85 (1993).
36. A. Blecka, G. Schaller, A. Maeder, *Nature* **360**, 320 (1992).
37. R. B. Leighton, *Nuovo Cimento Suppl.* **22**, 321 (1960).
38. R. K. Ulrich, *Astrophys. J.* **162**, 933 (1970).
39. J. Christensen-Dalsgaard, T. L. Duvall, D. O. Gough, J. W. Harvey, E. J. Rhodes, *Nature* **315**, 378 (1985); S. G. Korzennik and R. K. Ulrich, *Astrophys. J.* **339**, 1144 (1989).
40. A. N. Cox, J. A. Guzik, R. B. Kidman, *Astrosphys. J.* **342**, 1187 (1989).

41. C. A. Iglesias and F. J. Rogers, *ibid.* **371**, 408 (1991).
42. J. Christensen-Dalsgaard, D. O. Gough, M. J. Thompson, *ibid.* **378**, 413 (1991).
43. D. B. Guenther, P. Demarque, Y.-C. Kim, M. H. Pinsonneault, *ibid.* **387**, 372 (1992); J. N. Bahcall and M. H. Pinsonneault, *Rev. Mod. Phys.* **64**, 885 (1992); A. N. Cox and J. A. Guzik, *Astrophys. J.* **411**, 394 (1993).
44. C. R. Proffitt, *Astrophys. J.*, in press.
45. R. B. Stothers and C.-w. Chin, *ibid.* **348**, L21 (1990); *ibid.* **381**, L67 (1991); *ibid.* **390**, L33 (1992); *ibid.*, p. 136.
46. F. J. Swenson, G. S. Stringfellow, J. Faulkner, *ibid.* **348**, L33 (1990).
47. F. J. Swenson, J. Faulkner, F. J. Rogers, C. A. Iglesias, *ibid.*, in press.
48. S. Balachandran, *ibid.* **354**, 310 (1990).
49. C. A. Iglesias and F. J. Rogers, *ibid.* **412**, 762 (1993).
50. D. R. Alexander and J. W. Ferguson, personal communication; C. M. Sharp, in *Inside The Stars*, W. W. Weis and A. Baglin, Eds. (ASP Conf. Ser. 40, Astronomical Society of the Pacific, San Francisco, CA, 1993), p. 263.
51. D. Erskine, B. Rosznyai, M. Ross, *J. Quant. Spectrosc. Radiat. Transfer*, in press.
52. We thank A. N. Cox, D. Dearborn, C. R. Proffitt, and F. J. Swenson for helpful comments. Work performed under the auspices of the Department of Energy by the Lawrence Livermore National Laboratory under contract W-7405-Eng-48.

Astronomy and the Extreme Ultraviolet Explorer Satellite

Stuart Bowyer

The extreme ultraviolet wave band (100 to 912 angstroms) was thought until recently to be useless to astronomy, primarily because the opacity of the interstellar medium would prevent observations at these wavelengths. However, the interstellar medium has been found to be markedly inhomogeneous in both density and ionization state and the sun is fortunately located in a region of low extreme ultraviolet opacity. The Extreme Ultraviolet Explorer, launched in June 1992, has surveyed the sky in this wave band and has detected a wide variety of astronomical sources at considerable distances, including some extragalactic objects. Studies in the extreme ultraviolet band have already begun to increase our understanding of the contents of the universe.

Introduction

During the early years of the National Aeronautics and Space Administration (NASA), numerous studies were published attesting to the promise of astronomy from space. These reports pointed to the potential rewards of astrophysical research in virtually every band of the electromagnetic spectrum—with one exception. In an influential paper, Aller (*1*) argued a point that was almost self-evident given the knowledge base at that time. The great absorptive efficiency of extreme ultraviolet (EUV) radiation of even very small amounts of neutral hydrogen gas, combined with the ubiquitous distribution of this gas throughout the interstellar medium (ISM), would mean that astronomy at these wavelengths is impossible. Indeed, in the initial reports of the discovery of celestial x-ray sources, the (presumed) opacity of the ISM was used as an argument that the first source discovered, Scorpio X-1, must be radiating at wavelengths shortward of 4 Å (*2*). Subsequently, considerable work was carried out to calculate the absorption of the ISM at x-ray wavelengths, but there was no inclination to extend these calculations to wavelengths longer than 100 Å, much less to question Aller's basic conclusions.

In the ensuing years, a substantial number of satellites were launched to carry out astronomical research over the entire electromagnetic spectrum. In particular, numerous satellites were deployed to study the wavelength bands that bracket the EUV regime. At wavelengths shorter than the EUV region, the x-ray band (covering wavelengths from 1 to 100 Å) has been extensively surveyed by UHURU, SAS-C, Ariel IV, Ariel V, HEAO-1, Einstein, EXOSAT, Ginga, ROSAT, Yohkoh, and others. At longer wavelengths, the far ultraviolet band (covering wavelengths from 912 to ~3000 Å) has been observed with ANS, Copernicus, IUE, and the Hubble Space Telescope. The wavelengths between ~100 and 912 Å nominally constitute the EUV regime (the once-named "unobservable ultraviolet"). This band received scant attention. Only within the past 3 years have the long-standing pessimistic predictions concerning the ability to carry out astronomy at these wavelengths been truly tested. The result of these new efforts has been a surprising wealth of data covering a wide range of astronomical phenomena.

The first all-sky search for EUV sources was carried out with the British Wide Field Camera flown as part of the German ROSAT satellite. This survey covered part of the EUV bandpass (60 to 200 Å) and yielded a catalog of 384 sources (*3*). The first all-sky, all-EUV band survey has now been completed with the NASA Extreme Ultraviolet Explorer Satellite (EUVE) (*4*). A first catalog of 410 sources has been provided (*5*), and the total number of EUV sources that we estimate we will ultimately find in the data set runs well into the thousands. NASA has offered the scientific community the opportunity to use the spectrometers on EUVE as guest observers; some 270 research teams (one-third of them from outside the United States) have applied to use these facilities.

Why were the original projections for EUV astronomy so far off the mark and why does this field now look to be so productive? Several factors, in combination, have provided the basis for this change. The ISM has been discovered to be far different, and hugely more EUV transparent, than originally believed. New technology has been developed providing much higher sensitivity than was expected both in broad-band survey work and in spectroscopic capabilities. Finally, the EUV band has provided scientific bonuses not originally envisaged.

A variety of evidence garnered in the 1970s showed that the ISM was clearly not homogenous and that there was a marked deficiency of neutral interstellar gas in the sun's vicinity. The discovery of the diffuse soft x-ray background and interstellar O VI absorption indicated the presence of hot, ionized gas that would not contribute to the EUV opacity. The characterization of the ISM is far from clear [see (*6*) for a recent review], but all this work strongly suggests that the EUV opacity of the ISM within 1000 light years is far less than originally prophesized.

Dramatic proof of the viability of EUV astronomy was provided by a University of California at Berkeley EUV telescope flown as part of the Apollo-Soyuz mission in 1975. Bright EUV emission was detected from the hot, white dwarf star HZ 43 located at a distance of ~180 light years in the constellation of Coma Berenices (*7*). Three more sources were also discovered during this mission: the hot white dwarf Feige 24, the cataclysmic variable star system SS Cygni, and a late-type star, Proxima Centauri.

A major obstacle to the development of EUV astronomy was the lack of suitable technology. At visible, infrared, and ultraviolet wavelengths observations are usually made with telescopes whose mirrors collect the incoming photons in a "normal incidence" mode (that is, the light rays hit the mirror perpendicularly); the rays are subsequently brought to a focus and detected with film or an electronic detector. However, at wavelengths shorter than about 500 Å, normal incidence telescopes cannot be used because the photons are totally ab-

The author is professor of astronomy and director, Center for EUV Astrophysics, University of California, Berkeley, 2150 Kittredge Street, Berkeley, CA 94720.